

Dielectric Dispersion of New Ferroelectric Cobalt Halide Dimers: Bis-ethanolammonium-hexahalocobaltate, $(\text{C}_2\text{H}_8\text{NO})_2\text{Co}_2\text{X}_6$, $\text{X} = \text{Cl/Br}$

M. F. Mostafa and S. S. Arafat

Physics Department, Faculty of Science, University of Cairo, Giza, Egypt

Reprint requests to Dr. M. F. M.; E-mail: mohga@frcu.eun.eg

Z. Naturforsch. **55 a**, 595–604 (2000); received February 29, 2000

The AC conductivity in the frequency range 5.0 Hz - 10.0 kHz, the magnetic susceptibility in a field of 14.7 and $17.8 \cdot 10^4$ A/m, and differential thermal analysis at 78 K up to room temperature for bis-(ethanolammonium) Co_2X_6 , $\text{X} = \text{Cl}$ and Br are reported. The bromide dimer undergoes an order-disorder transition at 302 K and a displacive type ferroelectric transition at $T \sim 220$ K. The chloride dimer shows two transitions, the first being in a displacive ferroelectric one at $T \sim 210$ K showing critical slowing down. The second phase transition, occurring at 282 K, is found to be inactive in the electric measurements.

PACS: #76, 74

Key words: Dielectric Permittivity; Phase Transition; Ferroelectric Transition.

1. Introduction

Recent years have seen great interest in the study of magnetic interactions of transition metal salts [1], particularly cluster systems, with special interest in copper halide dimers [2]. To such systems belongs bis-ethanolammonium hexahalo-cuprate [3]. Room temperature structural analysis has indicated that the chloride and bromide salts form triclinic crystals. The structure consists of nearly planar $(\text{Cu}_2\text{Cl}_6)^{2-}$ dimers stacked to form infinite chains. The coordination of the Cu atoms is described as distorted square pyramidal with the ethanolammonium oxygen semicoordinated to the sixth coordination site for each copper atom. The copper compounds order antiferromagnetically at low temperature with ordering temperatures of 8 K and 77 K for the chloride and bromide dimers, respectively. More recently structural phase transformations have been observed in these compounds, and their electric behavior has been investigated [4]. The electric investigation of the bromide salt shows a very distinct transition at $T_{tr} = 245$ K. In order to investigate the role played by the metal halide anion on the structural and electrical properties, we have prepared the two new cobalt dimers, bis(ethanolammonium) hexa-chloro-di-cobaltate and bis(ethanolammonium) hexa-bromo-di-cobaltate, which will be referred to as ECOC and ECOB, respectively. In this article we

shall present the preparation, characterization, magnetic, thermal and electric behavior of the two cobalt dimers.

2. Experimental

2.1. Samples

The compounds were prepared by mixing equimolar ratios of ethanolammonium halide and the corresponding cobalt halide in acidified alcoholic solution. The mixture was kept at 80 °C for two hours, then cooled gradually to room temperature. Dark violet chloride salt and red violet bromide crystallites precipitated. The two compounds were recrystallized from a mixture of alcohol and ether then dried under vacuum. The chemical analysis showed the two compounds to have the correct chemical formulae.

2.2. Infra-red Spectroscopy

The IR spectra between 4000 to 100 cm^{-1} were obtained on an FTIR5000 spectrometer.

2.3. X-ray Experiment

The measurements were carried out on powdered samples at the x-ray diffraction center at the University of Cairo, using Ni filtered Cu-K α , $\lambda = 1.54184 \text{ \AA}$.

0932-0784 / 00 / 0600-0595 \$ 06.00 © Verlag der Zeitschrift für Naturforschung, Tübingen · www.znaturforsch.com



Dieses Werk wurde im Jahr 2013 vom Verlag Zeitschrift für Naturforschung in Zusammenarbeit mit der Max-Planck-Gesellschaft zur Förderung der Wissenschaften e.V. digitalisiert und unter folgender Lizenz veröffentlicht: Creative Commons Namensnennung-Keine Bearbeitung 3.0 Deutschland Lizenz.

Zum 01.01.2015 ist eine Anpassung der Lizenzbedingungen (Entfall der Creative Commons Lizenzbedingung „Keine Bearbeitung“) beabsichtigt, um eine Nachnutzung auch im Rahmen zukünftiger wissenschaftlicher Nutzungsformen zu ermöglichen.

This work has been digitalized and published in 2013 by Verlag Zeitschrift für Naturforschung in cooperation with the Max Planck Society for the Advancement of Science under a Creative Commons Attribution-NoDerivs 3.0 Germany License.

On 01.01.2015 it is planned to change the License Conditions (the removal of the Creative Commons License condition "no derivative works"). This is to allow reuse in the area of future scientific usage.

Table 1. Wave number (cm^{-1}) of the IR bands and their assignment for $[\text{C}_2\text{H}_7\text{NO}]\text{X}$ and $[\text{C}_2\text{H}_7\text{NO}]_2\text{Co}_2\text{X}_6$, $\text{X} = \text{Cl}/\text{Br}$ at room temperature.

$\text{C}_2\text{H}_7\text{-NOCl}$	$\text{C}_2\text{H}_7\text{-NOBr}$	$[\text{C}_2\text{H}_7\text{ONO}]_2\text{-Co}_2\text{Cl}_6$	$[\text{C}_2\text{H}_7\text{ONO}]_2\text{-Co}_2\text{Br}_6$	Assignment
3363	3290	3372	3423	OH-NH str.
3011	3051	3317	3379	C-H str.
2907	3051	2953	2977	N-H...X
2537	2568	2613	2912	N-H str.
2447	2438			
2318	2316			
2000	1989	2093, 1881	2036, 1864	C=O str.
1620	1616	1631, 1586	1617, 1575	N-H bend
1486	1478	1494, 1449, 1370	1470, 1359, 1315	C-H str.
1284	1282	1259	1253	OH-bend
1151	1156	1128	1123	C-N str.
1069	1065	1060	1056	C-N str.
982	970	999, 944	987, 936	C-N def.
825	837	838	838	C-H def.
857	860	852, 736, 690	850, 684	CH_2 -rock
		544	536	Co-O str.
404	369	492	441	C-N tor.
		321	302	Terminal Co-X str.
		241, 187	161, 116	Bridg. Co-X

2.4. Thermal Analysis

Differential thermal analysis (DSC) measurements were performed on a Shimadzu (50) differential scanning analyzer with a scanning speed of 5 K/min. The data were calibrated with the melting transition of Indium at 430 K.

2.5. Dielectric Measurements

The complex dielectric permittivity ε^* in the frequency range 5.0 Hz - 10.0 kHz was measured using a computer controlled lock-In amplifier type PAR 5207. The temperature was measured using a copper constantan thermocouple. The samples were measured in the form of pellets pressed under 2 tons/ cm^2 , each of 8 mm in diameter and 1.0 mm thick. The surfaces were coated with silver paste to ensure good electrical contact. The samples were first cooled to liquid nitrogen temperature; then the measurements were carried out while heating up the sample. The measuring technique and precautions to avoid stray capacitance are discussed in [5].

2.6. Magnetic Susceptibility Measurements

The magnetic susceptibility was measured using the Gouy method modified for low temperatures [6].

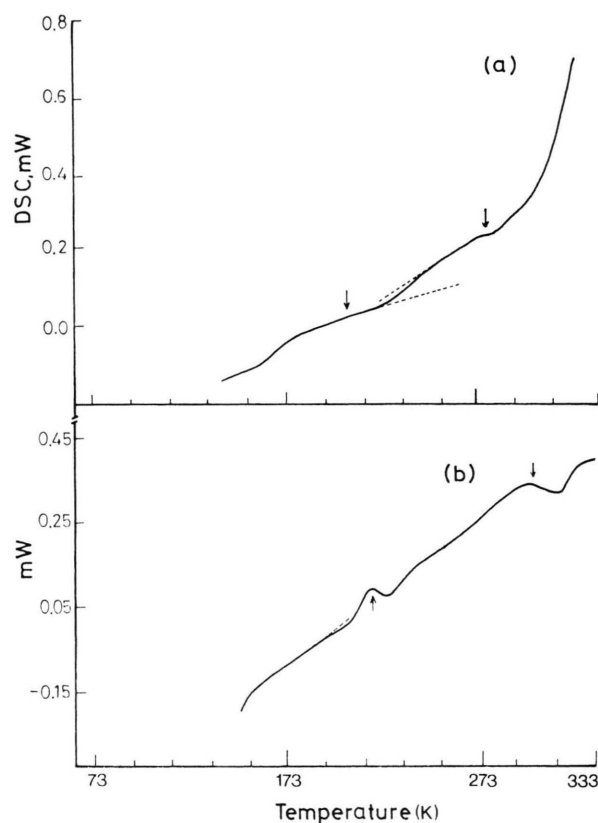


Fig. 1. (a) The DSC thermograph of ECOC; (b) DSC thermograph of ECOB.

Data were collected in magnetic fields of 14.7 and $17.8 \cdot 10^4 \text{ A/m}$, after cooling first to liquid nitrogen temperature, then taking measurements while heating up the samples. The error in the susceptibility measurements is less than 2%.

3. Results

3.1. Infrared Results

A list of the peaks and their assignment is shown in Table 1. The absorption bands at 321 and 303 cm^{-1} are due to Co-Cl and Co-Br terminal stretching, while those at 241, 187 and 213 and 161 cm^{-1} correspond to bridging Co-Cl and CoBr, respectively, indicating the formation of dimers [7].

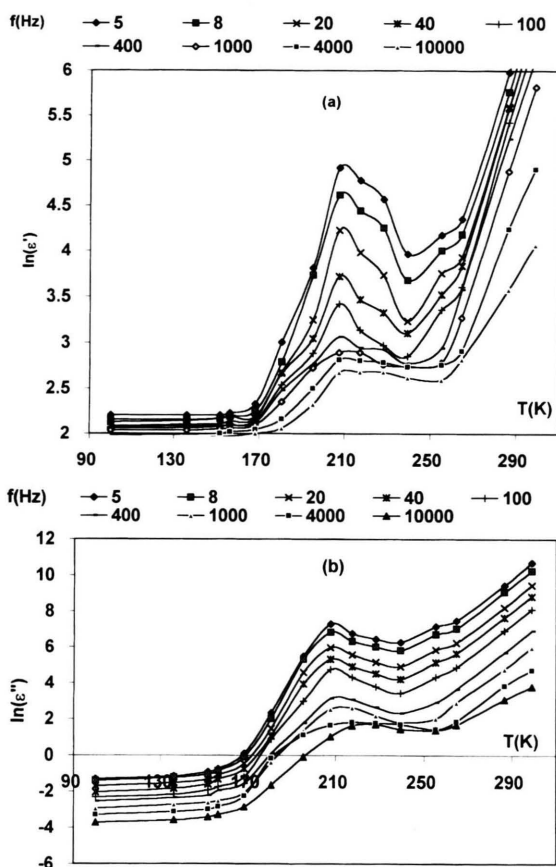
3.2. X-ray Diffraction Results

Preliminary x-ray powder diffraction showed that the two compounds are isomorphous to the corre-

Table 2. Thermodynamic parameters of $(C_2H_8NO)_2Co_2Cl_6$ and $(C_2H_8NO)_2Co_2Br_6$.

Compound	T (K)*	ΔH (J/mol)	ΔH (J/mol-deg)
ECOC	195.0	1186.4	5.92
	282.1	568.8	2.01
ECOB	217.29	1395.2	6.4
	301.16	3601.0	11.95

* Onset temperatures.

Fig. 2. The variation of the dielectric permittivity of ECOC in the temperature range 100 - 300 K at selected frequencies. (a) Real part $\ln \epsilon'$, (b) imaginary part $\ln \epsilon''$.

sponding copper compounds. The structure of the latter has been found to be triclinic with unit cell of dimensions $a = 0.6007$, $b = 0.8068$, $c = 0.8455$ nm, $\alpha = 67.99^\circ$, $\beta = 79.9^\circ$, and $\gamma = 78.77^\circ$ for the copper chloride salt, and $a = 0.6418$, $b = 0.826$, $c = 0.876$ nm, $\alpha = 68.17^\circ$, $\beta = 80.1^\circ$, and $\gamma = 78.5^\circ$ for the corresponding bromide salt [3].

3.3. Thermal Results

The differential thermal analysis (DSC) thermograph obtained in the temperature range 78 - 333 K for the chloride (ECOC) salt shows no real sharp peaks, but a change in the rate of heat flow with temperature at $T \sim 195$ K, as seen in Fig. 1(a), reflecting a second order phase transition. A very small anomaly with an onset temperature of 282 K is also observed. It is to be mentioned that the enthalpy and the calculated entropies are small, as seen from Table 2.

Figure 1(b) shows the DSC thermograph for ECOB. It depicts a change in the slope at 206 K followed by an endothermic peak with initiation temperature at $T_1 \simeq 217.29$ K. At $T_2 = 301.16$ K an endothermic peak with a low temperature tail is observed. The thermodynamic parameters are listed in Table 2.

The large value of the entropy of ~ 12 kJ/mole-K obtained at 301 K for the bromide reflects an order-disorder type transition [8]. The very small value of the entropy is an indication for a continuous transition. We shall assign values of $\Delta S \sim 6$ J/mole-K to a displacive type transformation. This will be confirmed from the dielectric measurements.

3.4. Dielectric Permittivity Results

3.4.1. Bis-ethanolammonium-hexachloro-cobaltate (ECOC)

The variation of the real (ϵ') and the imaginary (ϵ'') part of the dielectric permittivity as function of temperature on a semilogarithmic scale is shown in Fig. 2 for the ECOC dimer. ϵ' is temperature and frequency independent up to $T \sim 170$ K, where it starts to increase reaching a maximum at 210 K. This is followed by a gradual decrease up to ~ 240 K, a strong dispersion is observed beyond this temperature which increases as T increases and f decreases. A closer look at the peak ($\epsilon'-T$), as depicted in Fig. 3(a), shows its complex structure, with almost two split peaks, whose width becomes broader with increasing frequency. Similar behavior is noted for the imaginary part ϵ'' as seen in Fig. 3(b), where the maximum values of ϵ'' decrease and the peaks show a slight shift towards the high temperature side as frequency increases. These results represent the dielectric response characteristic of a para-ferroelectric phase transition of second order, where critical slowing down of the ferroelectric order parameter fluctuation is observed [9].

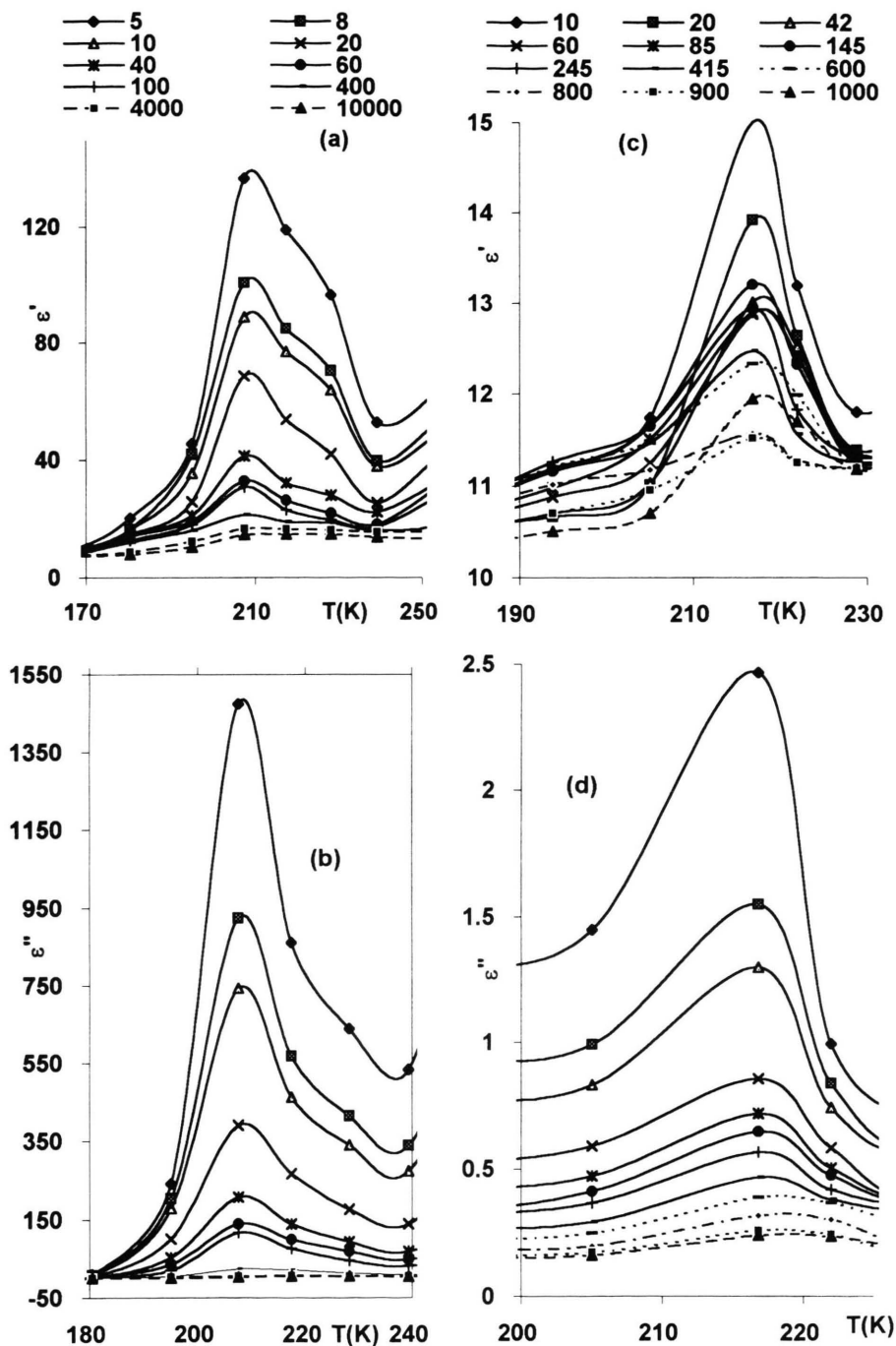


Fig. 3. The variation of the dielectric permittivity of ECOC and ECOB near the transition temperature at selected frequencies. (a) ECOC, real part $\ln \epsilon'$. (b) ECOC, imaginary part $\ln \epsilon''$. (c) ECOB, real part $\ln \epsilon'$. (d) ECOB, imaginary part $\ln \epsilon''$.

3.4.4.2. Bis-ethanolammonium-hexabromocobaltate (ECOB)

The variation of ϵ' and ϵ'' as function of the temperature on a semilogarithmic scale is shown in Figure 4.

In contrast to ECOC, the real part of the permittivity continuously increases with increasing temperature and is frequency dependent. A change in the rate of increase is observed at 206 K followed by a distinct peak at 219 K as depicted in Figure 4a). The anomaly

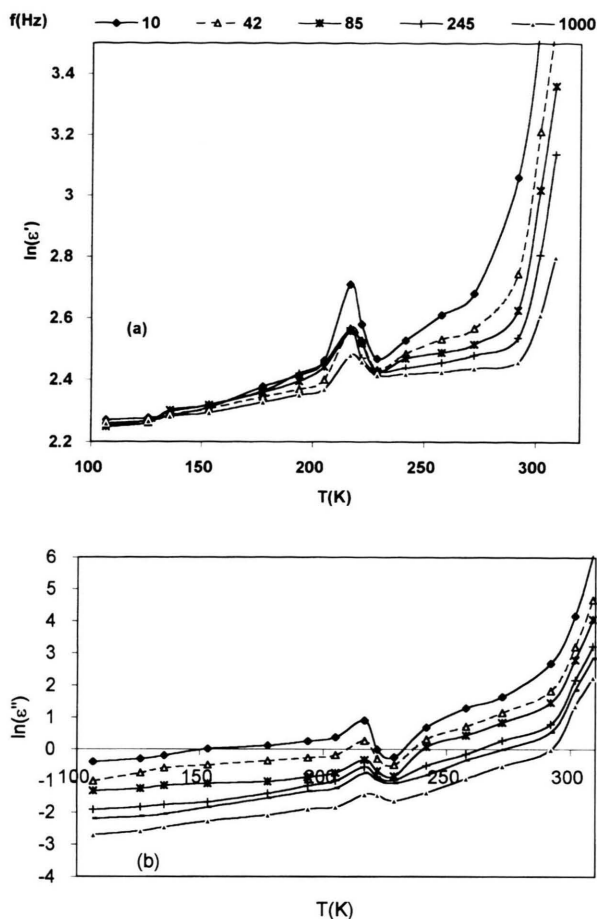


Fig. 4. The variation of the dielectric permittivity of ECOB in the temperature range 100 - 300 K at selected frequencies. (a) Real part $\ln \epsilon'$, (b) imaginary part $\ln \epsilon''$.

seems to occur at the same temperature, ~ 219 K, within experimental accuracy for the range of frequencies studied. It is to be noted that an inflection point is observed at ~ 300 K, which is rather prominent in the ϵ'' - T graph. Also ϵ^* , (as seen in Fig. 3(c) and (d)), does not exhibit the characteristic split peak seen in Fig. 3(a) and (b). The observed temperature dependence of ϵ' allows to doubt if we are dealing with a continuous phase transition in ECOB.

3.5. Magnetic Susceptibility Results

The corrected molar magnetic susceptibility χ_M as function of temperature for ECOC and ECOB is shown in Fig. 5(a) and 5(b). Correction for diamagnetism was carried out using Pascal's table. The sus-

Table 3. Effective magnetic moment and Curie constants for the $[\text{C}_2\text{H}_8\text{ONO}]_2\text{Co}_2\text{X}_6$, X = Cl/Br in different temperature ranges.

Compound	Temperature range (K)	μ_{eff} (BM)	Curie constant θ (K)
ECOC	(I) $T > 240$	4.51 ± 0.04	40 ± 7
	(II) $150 < T < 200$	4.65 ± 0.03	20 ± 8
ECOB	(I) $T > 300$	4.83 ± 0.05	85 ± 15
	(II) $240 < T < 290$	4.33 ± 0.05	50 ± 7
	(III) $150 < T < 210$	4.31 ± 0.05	65 ± 10

ceptibility decreases with increasing temperature, as is expected for Curie-Weiss type behavior. However, at temperatures $T < 150$ K, a field dependent susceptibility is observed for ECOB, with a lower value of χ at the higher measuring field. This can most likely be attributed to short range magnetic interaction, which usually precedes long range ordering. Thus we expect magnetic ordering to occur at a temperature lower than that of liquid nitrogen. In contrast to ECOB, the chloride dimer does not show any field dependent susceptibility at low temperature. This is consistent with the fact that bromide compounds undergo magnetic transitions at a temperature higher than their corresponding chloride [3].

Besides the field dependent susceptibility noted at low temperature, anomalies in the temperature region 200 - 225 K were observed for both dimers (see Fig. 5(b)). On one hand, ECOC shows a region of temperature independent susceptibility that extends over a range of ~ 15 K. On the other hand, ECOB shows a small peak of $\sim 8\%$ high above the susceptibility background. The peak decreases in height as the measuring field increases, with no apparent change in its position. This behavior is typical for first order structural transitions [10, 11], as has previously been found in almost all of the structural transitions of the alkylammonium metal complexes studied in our laboratory [6, 10, 11].

Least squares fitting of the susceptibility vs. $1/(T - \theta)$ with θ as a varying parameter were performed for the two compounds above and below the transition temperature. It yields the effective magnetic moments and Curie-Weiss constants listed in Table 3. The obtained values are as would be expected for high spin Co^{+2} in a distorted octahedral symmetry. The small differences in the effective magnetic moments obtained below and above the transition temperatures reflect the slight changes in the distortion around the Co^{+2} as a result of structural transformation.

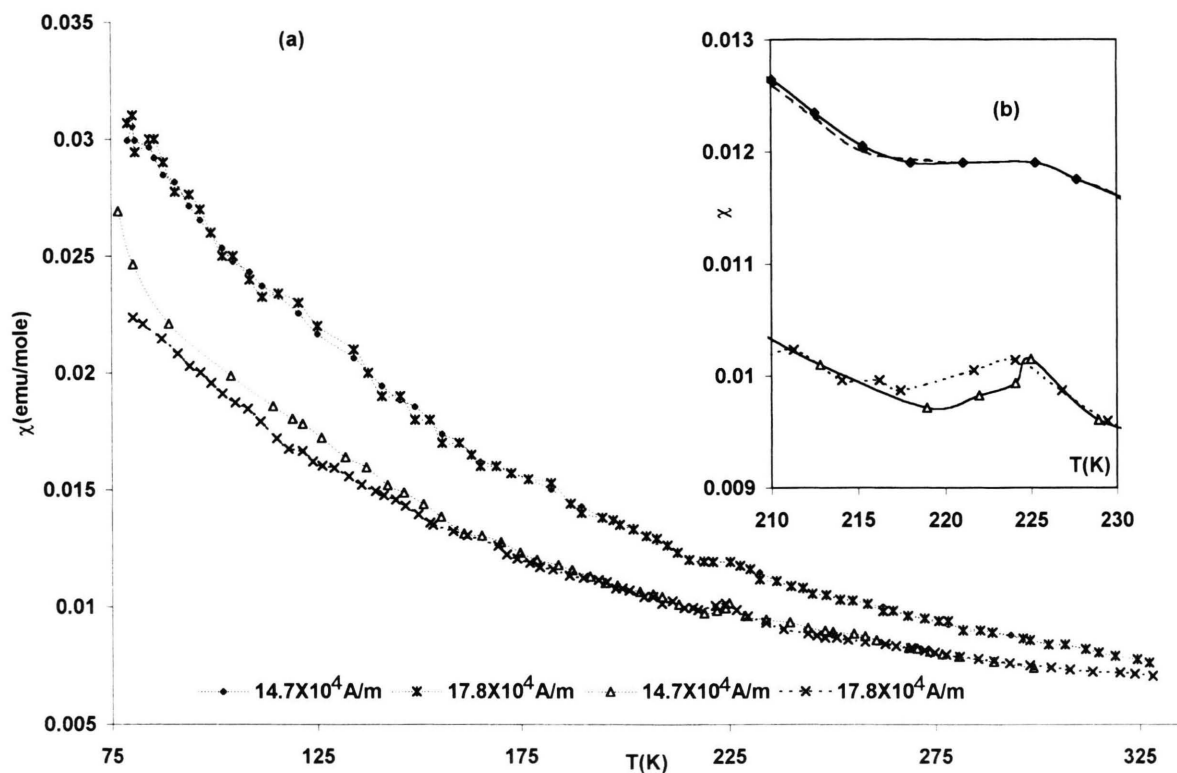


Fig. 5. (a) Corrected molar magnetic susceptibility (χ_M) between liquid nitrogen and room temperature at magnetic fields of 14.7 and 17.8×10^4 A/m for ECOC and ECOB. (b) Corrected molar magnetic susceptibility (χ_M) in the temperature range 210 - 230 K.

4. Discussion

The temperature dependence of the dielectric properties of the two dimers will be discussed in two parts. The first part deals with the dielectric anomaly observed below and near the ferroelectric transition temperatures of 210 and 219 K, respectively. The second part deals with the high dielectric constant observed at temperatures well above these temperatures. Its frequency dependence will be explained in terms of the dielectric modulus.

4.1. Dielectric behavior near T_c .

Preliminary powdered X-ray diffraction obtained on ECOC and ECOB at room temperature shows that they are isomorphous to the corresponding copper complexes. At the present stage of knowledge, particularly when no information about the crystal structure at low temperature is available, little can be said about the reason for the observed differences in the

two compounds. However, qualitatively, several reasons are suggested to account for their differences. These are:

(i) Effect of magnetic interaction on the dielectric constant.

Magnetic susceptibility results have indicated that the ECOB exhibits short range magnetic interactions at low temperatures, thus the exchange interaction between the ions will be altered by the applied electric field. This interaction between the modulated field and the magnetic exchange interaction will affect the dielectric constant. According to Hatta and Sugimoto, for an antiferromagnetic material with Néel temperature T_N , the dielectric constant is given by [12]

$$\varepsilon' = a|t| \ln |t| + b + c|t|, \quad (1)$$

where a , b , and c are constants and $t = (T - T_N)/T_N$. This shows that in an antiferromagnetic material, the dielectric constant is an increasing function of temper-

ature as is clearly seen for ECOB in the low temperature region. This may explain the observed behavior of ϵ' - T relation at low temperature. It also would explain the temperature independent ϵ' found for ECOC at low temperatures, since this does not show any short range interaction near liquid nitrogen temperature.

(ii) Mechanism of phase transition in the 200 - 220 K region.

As can be seen from the magnetic magnetic behavior at 210 - 220 K, it is different for the two dimers, as are the DSC results. Thus the mechanism of phase transitions in the two dimers must be different, which will affect the permittivity dependence.

(iii) Effect of atomic size of the halide ion.

The effect of the atomic size is likely to contribute to the dielectric constant not only at $T < 200$ K but also over the whole temperature range. As would be expected, when the larger size Br ion replaces a Cl ion, the molar volume increases, hence the space available for the motion of the polar ethanolammonium ion becomes larger.

(iv) Strength of the N-H...X bond.

This would also account for the differences in the (ϵ' - T) relation over the whole temperature range. The difference in the strength of the N-H...Cl and N-H...Br bonds resulting from the difference in the electronegativity of the two halide ions with chloride being more electronegative than bromide will affect the strength of the NH...X bond. Since the phase transformation is associated with breakage of the hydrogen bonding.

4.2. Complex Dielectric Modulus

It can be seen from Figs. 2(b) and 4(b) that the two dimers are highly lossy. Figures 6 and 7 show the modulus plots of ECOC and ECOB, respectively. It can be seen that the centers of these arcs lie below the M' -axis, the angle α gives an indication of the broadness of the frequency dependence of the imaginary part of the dielectric modulus [13]. The fact that the modulus plots follow semicircular arcs, indicates that a considerable contribution to the permittivity comes from the conductivity at high temperatures.

We have used the complex modulus plots to obtain the values of α and ϵ_∞ in different temperature regions for the two dimers as listed in Table 5. Values of $\alpha \sim 0.1$ reflect the monodispersive nature of

Table 4. The angle α and ϵ_∞ at different temperatures.

Compound	Temperature range (K)	α	ϵ_∞
ECOC	195 - 207	0.15 - 0.18	14.7 - 16.1
	217 - 255	0.1 - 0.12	
	265 - 298.9	0.22 - 0.26	16.7 - 208
ECOB	228 - 257	0.07 - 0.13	11.1 - 11
	272 - 308	0.35 - 0.27	11.2 - 12.5

the two dimers at temperatures higher than the ferroelectric transition temperatures. Relaxation times (τ) were determined from $\omega\tau = 1$, and a plot of the relation between $\ln(\tau)$ and reciprocal temperature as seen in Fig. 8 yields activation energies of 0.047 and 0.026 eV for the relaxation process for ECOC and ECOB, respectively.

The phase transition in these two dimers is a result of the thermal motion of the ethanolammonium ion. This causes a change in the N-H...X bonding between the substituted ammonium cation and the halide ion. This type of motion has been found in many alkyl and alkylene ammonium transition metal complexes [14]. The molecular mechanisms of the phase transformation found in these dimers seem to be different from each other. The bromide dimer undergoes an order-disorder phase transition above 302 K. This is characterized by a large entropy effect $\Delta S = 2 R \ln 2 = 11.53$ J/mole-K. Another phase transition, probably of first order and associated with smaller entropy changes ($\Delta S = 5.7$ J/mole-K), occurs at 219 K. The chloride dimer (ECOC) undergoes a displacive type ferroelectric transition showing critical slowing down of the dipoles at 210 K, which is associated with an entropy change of $\Delta S = 5.9$ J/mole-K. The two displacive transitions probably have their origin in the deformation of the inorganic sublattice. We propose that three phases exist in the temperature range between 300 K and that of liquid nitrogen for the two dimers. A high temperature phase (I) for $T > 280$ K, an intermediate temperature phase (II) ($230 \text{ K} < T < 280 \text{ K}$) and a low temperature phase (III) for $T < 200$ K. The differences in the dielectric, and magnetic properties of the two compounds may be related to the differences in molecular interactions as Br ion replaces the Cl ion. The energy of the hydrogen bonding of N-H...Cl must be different from that of the N-H...Br. This may be due to the ion size and electronegativity which would cause steric effects. It can be suggested that due to the large size of the Br ion the space available for the rotational motion of

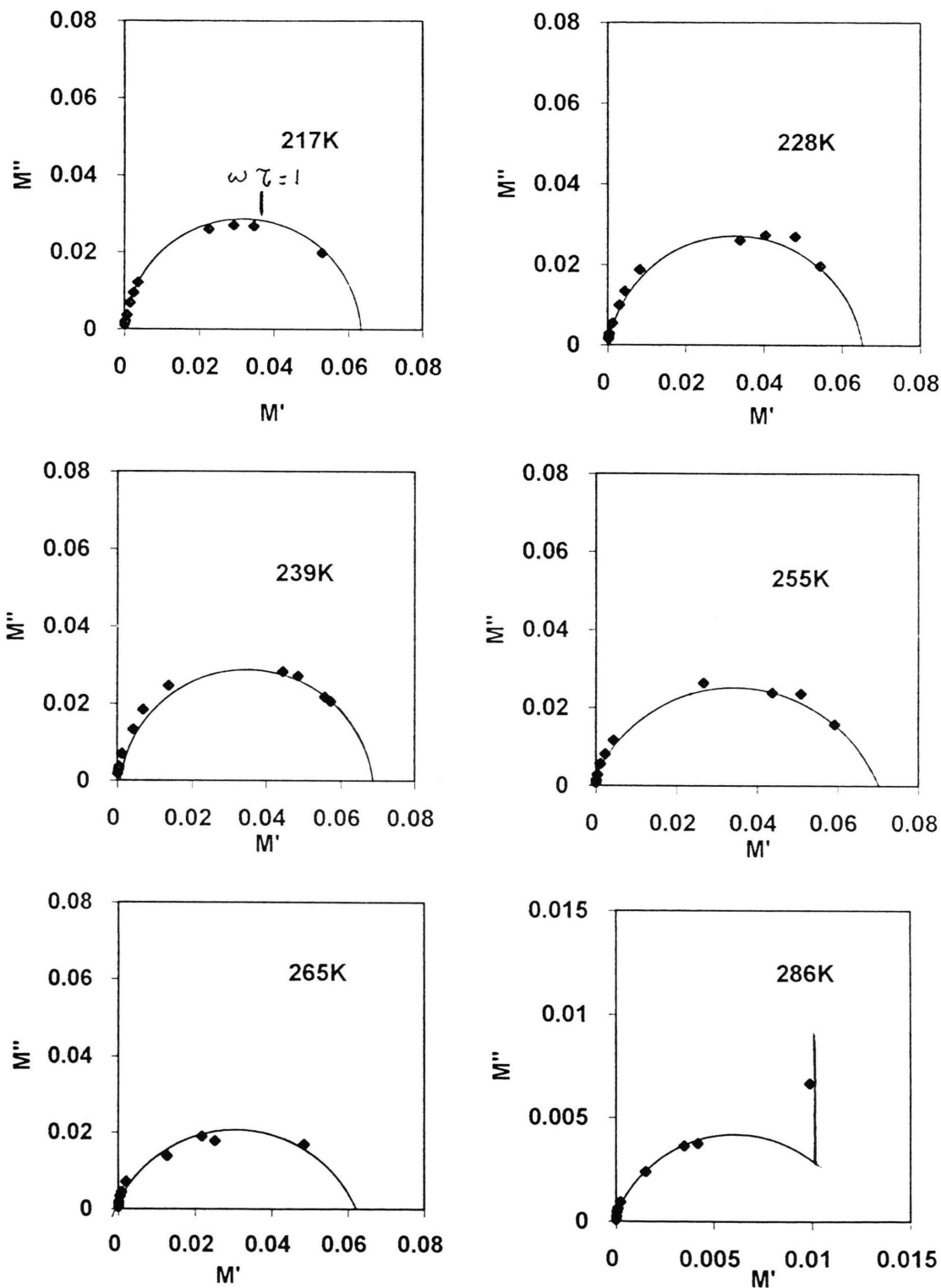


Fig. 6. The dielectric modulus at different temperatures for ECOC.

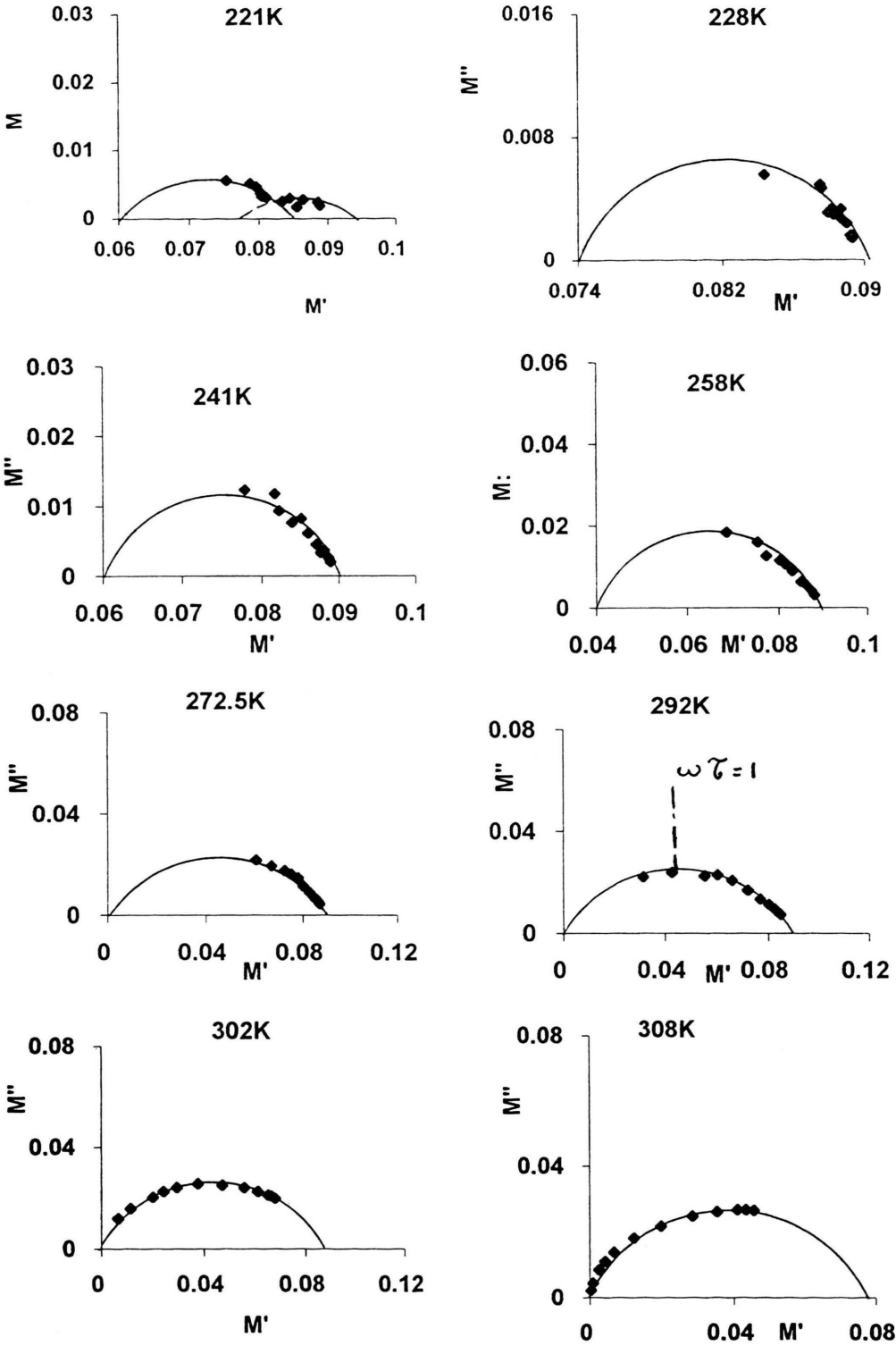


Fig. 7. The dielectric modulus at different temperatures for ECOB.

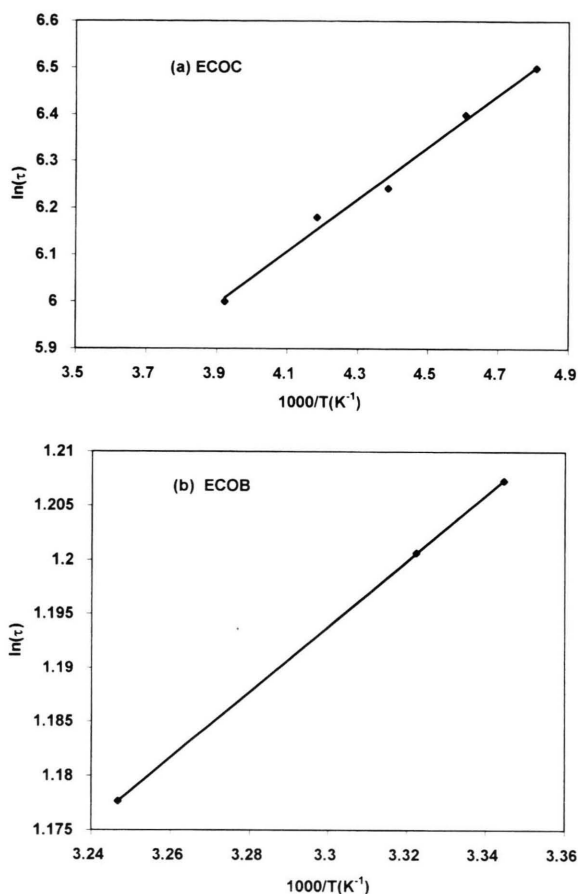


Fig. 8. $\ln(\tau)$ vs. $1000/T$ for (a) ECOC, (b) ECOB.

the organic ion will increase compared to the chloride dimer. Also the energy of interaction will be different in the two cases. The difference in the mechanism of the phase transition may also be due to the difference in the number of relaxators.

5. Conclusion

The dielectric permittivity, DSC and magnetic susceptibility investigations of the two newly prepared ECOC and ECOB have indicated that:

1. The dielectric dispersion of ECOC shows a dispersive type ferroelectric phase transformation with critical slowing down in the 200 K range.
2. The small value of the entropy rules out an order-disorder type transition.
3. The dielectric dispersion of the ECOB shows a ferroelectric phase transformation of the first kind at 219 K.
4. An order disorder type transition is also found at 301.8 K for ECOB.
5. The replacement of the chloride by the larger and less electro-negative ion Br^- causes a change in the phase transition mechanism, indicating the important role played by the metal halide ion.

- [1] L. J. DeJongh and A. R. Miedema, *Adv.Phys.* **23**, 1 (1974).
- [2] R. Carlin and A. J. Van Duyneveldt, *Magnetic Properties of Transition Metal Compounds*, Springer-Verlag, New York 1981, p. 77.
- [3] B. Scott and R. D. Willett, *Inorg.Chem.Acta* **141**, 139 (1988).
- [4] M. F. Mostafa, S. S. Arafat, and M. M. Abdel-Kader, *Phil.Mag.* **75B**, 167 (1997).
- [5] M. F. Mostafa, M. El-Nimer, and F. Richa, *Phys. Scripta* **43**, 451 (1993).
- [6] M. F. Mostafa, M. A. Semary, and M. A. Ahmed, *Physica* **68-88B**, 691 (1976).
- [7] D. M. Adams and P. J. Lock *J. Chem. Soc. A*, 620 (1967).
- [8] R. Jakubas, G. Bator, M. Foulon, J. Lefebvre, and J. Matuszewski, *Z. Naturforsch.* **48a**, 529 (1993).
- [9] K. Yoshimitsu, K. Matsubara, and T. Matsubara, *Progr. Theor. Phys. Suppl.* 109 (1968).
- [10] M. F. Mostafa, M. Abdel-Kader, A. S. Atallah, and M. El-Nimer, *Phys. Stat. Sol. (a)* **135**, 549 (1993).
- [11] M. F. Mostafa, M. M. Abdel-Kader, S. S. Arafat, and E. M. Kandeel, *Phys. Scripta* **43**, 627 (1991).
- [12] I. Hatta and N. Sugimoto, *J. Phys. Soc. Japan* **49**, 1000 (1980).
- [13] P. B. Macedo, C. T. Moynihan, and R. Bose, *Phys. Chem. Glass* **13**, 171 (1972).
- [14] A. Wolthuis, W. J. Huiskamp, L. J. DeJongh, and R. L. Carlin, *Physica* **42B**, 301 (1986).